*Biochimica et Biophysica Acta*, 1029 (1990) 274–284
Elsevier

BBAMEM 75039

# The pH dependence of the cardiac sarcolemmal $Ca^{2+}$-transporting ATPase: evidence that the $Ca^{2+}$ translocator bears a doubly negative charge

Deborah A. Dixon and Duncan H. Haynes

*Department of Pharmacology, University of Miami School of Medicine, Miami, FL (U.S.A.)*

(Received 16 January 1990)
(Revised manuscript received 6 July 1990)

Key words: Calcium pumping ATPase; Transport ATPase; ATPase; Ion transport; Heart; Sarcolemma; Sarcoplasmic reticulum

**The pH dependence of the $Ca^{2+}$-transporting ATPase of bovine cardiac sarcolemma was determined in a membrane vesicle preparation. The maximal velocity ($V_{max}$) at saturating external $Ca^{2+}$ showed a sigmoidal pH dependence with maximal values in the 6.0–6.5 range, a half-maximal value at 7.2 and minimal ($\leq$ 15%) values at pH $\geq$ 8.0. The apparent affinity for $Ca^{2+}$ ($1/K_m$) varied over $10^4$-fold for 6.0 $\leq$ pH $\leq$ 8.5, increasing with increasing pH. Plots of log($1/K_m$) vs. pH were biphasic. In the acid range (6.0 $\leq$ pH $\leq$ 7.2), a slope of 2.6 was observed for the calmodulin-activated form of the pump. For 7.2 $\leq$ pH $\leq$ 8.5, a slope of 0.5 was observed. At pH 7.4, the $K_m$ is approx. 48 $\pm$ 19 nM. The $Ca^{2+}$ pump of cardiac sarcoplasmic reticulum in the same preparation had a $K_m$ of 304 $\pm$ 115 nM and showed a similar pH dependence except that the slope in the acid range was 1.7. When calmodulin was removed from the sarcolemmal pump, its $K_m$ was raised to approx. 1.0 $\mu$M, the slope in the acid range was reduced to 1.7 and the $V_{max}$ was markedly reduced. The results are explicable in terms of a model in which each of the two $Ca^{2+}$ binding sites on the pump contains two buried $COO^-$ groups responsible for high affinity. The $K_m$ effect is explained by 2 $H^+$ vs. 1 $Ca^{2+}$ competition for occupation of each of the two cytoplasmically-oriented translocators (4 $H^+$ vs. 2 $Ca^{2+}$). The $V_{max}$ effect is explained by counter-transport of $H^+$. The findings are considered in terms of the published amino acid sequence of the cardiac sarcolemmal pump and recent site-directed mutagenesis vs. function studies identifying the $Ca^{2+}$ binding site in the skeletal sarcoplasmic reticulum pump. The kinetic data are also applied to pump behavior under conditions of ischemia and acidosis.**

## Introduction

The cyclic rise and fall of cytoplasmic $Ca^{2+}$ levels serves as the primary determinant of the contraction/relaxation cycle in heart. This is the result of the interplay between the sarcoplasmic reticulum (SR) and the sarcolemma (SL). The $Ca^{2+}$ release mechanism of the cardiac SR has been well-elucidated by in situ studies in skinned cardiac Purkinje cells [1]. Both the SR and the SL membranes have $Ca^{2+}$-ATPase pumps responsible for $Ca^{2+}$ sequestration and extrusion, respectively. Biochemical characterization and active transport studies in cardiac SR and SL vesicles show a basic similarity between the two pumps but have also uncovered distinct differences [2–5]. The SL membrane also contains a $Na^+/Ca^{2+}$ exchanger which contributes to the $Ca^{2+}$ extrusion process [6,7] during its early phase [5] when the cytoplasmic $Ca^{2+}$ concentration ($[Ca^{2+}]_{cyt}$) is high. Understanding the pH-dependent interplay between these systems is important to our understanding of the behavior of the beating heart in acidosis and ischemia [8–11].

The present communication focuses on the pH dependence of the cardiac SL pump. Specifically, it gives evidence that the high-affinity $Ca^{2+}$ binding (transloca-

Abbreviations: SR, sarcoplasmic reticulum; SL, sarcolemma; PM, plasma membrane of non-muscular origin; $[Ca^{2+}]_{cyt}$, concentration of free $Ca^{2+}$ in the cytoplasm; $[Ca^{2+}]_o$, free $Ca^{2+}$ concentration in solution external to vesicle; $[Ca^{2+}]_i$, free $Ca^{2+}$ concentration in vesicle lumen; $V_0$, maximal rate of increase of $[Ca^{2+}]_i$ in the initial phase; $V_{max}$ and $SS_{max}$, maximal rate or $[Ca^{2+}]_i$ (respectively) at steady-state with saturating $[Ca^{2+}]_o$; $K_m$, $[Ca^{2+}]_o$ giving half-maximal rate or $[Ca^{2+}]_i$ in steady state; CTC, chlorotetracycline; Tris, tris(hydroxymethyl)aminomethane; Hepes, 4-(2-hydroxyethyl)-1-piperazineethanesulfonic acid; EGTA, ethylene glycol bis($\beta$-aminoethyl ether)-*N*,*N*′-tetraacetic acid; CAM, calmodulin.

Correspondence: D.H. Haynes, Department of Pharmacology (R. 189), P.O. Box 016189, University of Miami School of Medicine, Miami, FL 33101, U.S.A.

tor) sites contain $COO^-$ groups and that 4 $H^+$ compete with 2 $Ca^{2+}$ to occupy these sites. The present experimentation is based on studies of rabbit skeletal SR which will be reviewed briefly.

*Evidence for $COO^-$ groups in high-affinity $Ca^{2+}$ binding sites of skeletal SR $Ca^{2+}$-ATPase*

The earliest evidence that the high-affinity $Ca^{2+}$ binding site of skeletal SR $Ca^{2+}$-ATPase contains $COO^-$ was given by experimentation of Murphy published in 1980 [12]. In these studies, rabbit skeletal SR was treated with alkyl carbodiimides and a class of $COO^-$ group was characterized as essential for $Ca^{2+}$-dependent phosphorylation of the $Ca^{2+}$-ATPase. The class was protected by $Ca^{2+}$ with an $EC_{50}$ of 6 $\mu$M and a Hill coefficient of 2.1 (at 0 °C). The reactivity vs. pH profile showed a sigmoidal shape (as in Fig. 1 of the present study), with a midpoint value of 6.4. Stoichiometric analysis showed that covalent modification of one $COO^-$ per pump molecule was sufficient for full inactivation. The agreement between the transport and inactivation analysis is striking, particularly when the differences in temperature and possible differences in enzyme distribution in the two states are considered.

In 1983 our laboratory presented a kinetic study of the $Ca^{2+}$-ATPase of rabbit skeletal SR showing direct competition between $Ca^{2+}$ and $H^+$ for binding to the high-affinity $Ca^{2+}$ binding site [13]. This was based on an approximately three-order-of-magnitude increase in the $K_m$ for $Ca^{2+}$ as the pH was decreased from 7.0 to 5.5. This was taken as evidence that each of the two high-affinity binding site contained two negative charges, identified as buried $COO^-$ groups with $pK_a$ values of approx. 7.2 [13]. The amino acid sequence of the enzyme, deduced from its complementary DNA sequence, was published by MacLennan et al. [14] in 1985. Recently Clark et al. [15] used site-directed mutagenesis to identify amino acids critical to high-affinity $Ca^{2+}$ binding-dependent phosphorylation of the same enzyme. Their experiments identified the following amino acids as critical to high-affinity binding: Glu-309, Glu-771, Asn-796, Thr-799, Asp-800 and Glu-908. The three glutamates and one aspartate contribute a total of four negative charges. This confirms our deduction that 4 $H^+$ compete with 2 $Ca^{2+}$ for occupancy of the high affinity site [13].

Earlier studies from our laboratory have suggested that protonation/deprotonation reactions are important for expulsion of $Ca^{2+}$ into the SR lumen [16]. Analysis of the pH dependence of the $V_{max}$ suggested competition between $H^+$ and $Ca^{2+}$ for occupation of the lumenally-oriented, low-affinity form of the $Ca^{2+}$ binding site [13]. Lower pH increased the $V_{max}$. Computer modelling showed that the effect could be explained by $H^+$ aiding in the release of transported $Ca^{2+}$ and serving as a counter-transported ion [13,17,18]. From the physiological point of view, it is important to understand the pH dependence of these pumps. An example is the problem of acidosis in beating heart [8–11].

The present communication reports a similar study of the cardiac SL and SR pumps. These pumps are more complicated than the skeletal SR pump. Both cardiac pumps are regulated by calmodulin (CAM) and by cAMP stimulated phosphorylation, showing differing kinetic properties in their several states. In the remainder of this section the properties of the two cardiac pumps relevant to the present experimentation will be briefly reviewed.

*Cardiac SR pump*

The pH dependence of $Ca^{2+}$ transport by cardiac SR has not been systematically studied, although the pH dependence of the phosphorylation and dephosphorylation reactions at high external $Ca^{2+}$ has been reported [19]. The transport rate at saturating external $Ca^{2+}$ has been shown to increase with decreasing pH [20] but the pH dependence of the $K_m$ is not known. The canine cardiac SR pump has a $K_m$ of 0.86 $\mu$M in the unactivated state [21]. Activation by a CAM-dependent protein kinase reduces the $K_m$ to 0.61 $\mu$M [21]. There is also evidence for a 3-fold increase in $V_{max}$ via a direct effect of CAM [22]. Cyclic-AMP-dependent (phospholamban, Ref. 23) phosphorylation has also been shown to lower the $K_m$ for $Ca^{2+}$ to 0.62 $\mu$M [24] and to increase the maximal rate [25,26]. Dual activation reduced the $K_m$ to 0.42 $\mu$M. It is noted that this final $K_m$ value is six times as large as that of rabbit skeletal SR, which does not share these features of regulation. The amino acid sequence of the cardiac SR is identical to that of skeletal SR about the six residues comprising the proposed high affinity $Ca^{2+}$ binding sites (compare Ref. 27 with Ref. 14 using Ref. 15). The present study reports the apparent $Ca^{2+}$ affinity of high-affinity binding site for bovine cardiac SR, describes $H^+/Ca^{2+}$ competition for this site, and considers the results in terms of the above primary structural information.

*Cardiac SL pump*

The cardiac SL pump [2,28] is stimulated by CAM and by cAMP-dependent phosphorylation [3,4]. The most dramatic of these effects is the CAM-induced increase in $Ca^{2+}$ affinity and rate of the pump. In bovine cardiac SL, this process reduces the $K_m$ from 1.8 $\mu$M to 64 nM [29]. The latter value is about a factor of five lower than the $K_m$ for the SR of the same tissue. The present study concentrates on the CAM-stimulated form of the SL pump. The amino acid sequences of CAM-sensitive, sarcolemmal $Ca^{2+}$-ATPases of skeletal and cardiac origin have been determined [30]. The amino acid sequence for the erythrocyte plasma membrane $Ca^{2+}$-ATPase has also been published [31]. This infor-

mation will be considered together with the information on the composition of the high-affinity site in skeletal SR [15] and with the present observations on the pH dependence of its apparent $Ca^{2+}$ binding constant.

## Materials and Methods

Preparation of bovine cardiac sarcolemmal (SL) vesicles and the quantitative aspects of the measurement of their $Ca^{2+}$ transport were as described previously [29]. All active transport reactions were measured at 37 °C using 30 μg/ml SL vesicles with 10 μM chlorotetracycline (CTC) in a $Na^+$-free solution consisting of 100 mM KCl, 250 mM sucrose to provide osmotic buffering, 0.1 mM $MgCl_2$ and buffer at 25 mM. For experimentation in the pH range 7.0–8.5, the buffer was 25 mM Tris + 25 mM Hepes adjusted with HCl or KOH. For pH < 7.0, imidazole was substituted for Tris. Tests at pH 7.0 showed that this substitution did not affect the transport reaction. Adequacy of the buffers and constancy of the set pH values was verified by pH readings in the cuvettes at the end of selected runs. Calibrations [32,33] of fluorescence vs. internal lumenal $Ca^{2+}$ concentration ($[Ca^{2+}]_i$) were made at each pH studied.

Before measurement of active uptake, the SL vesicles were preincubated with 5 μM calmodulin at free $Ca^{2+}$ concentrations defined by a $Ca^{2+}$/EGTA buffer ($[EGTA]_T = 2.5$ mM) and at the stated pH. As described previously [13], the constants of Martell and Smith [34] were used to define $[Ca^{2+}]_0$ as a function of the $Ca^{2+}$/EGTA ratio and pH. In the present study, the preincubations were for one hour. Control experiments showed that the transport rate were independent of preincubation time for 15–60 min. Also, experiments showed that the transport rates measured at pH 7.4 were not affected by previous exposure to pH 6.0 or 8.5. In experiments directed at the basal state of the SL pump, the calmodulin was omitted and 1.0 μM soluble troponin-I was substituted [29].

The active transport reaction was initiated by the addition of 2.0 mM Mg-ATP. The maximal rate in the initial phase ($V_0$) and maximal uptake at steady state ($SS_{max}$) were determined as described previously [29]. The presented data are for the inside-out fraction of the SL vesicles which is capable of ATP-supported transport. The rate data are expressed in units of millimoles of free $Ca^{2+}$ per liter of vesicle volume per min (mM/min). These can be converted into nmol/mg protein per min using the trapped sucrose volume of 2.2 μl/mg. All presented data are the average of three determinations with three separate preparations. The rate data were not influenced by passive leakage of $Ca^{2+}$ which is very slow in these preparations [29]. In the present study, the half-time for passive $Ca^{2+}$ equilibration was $\geqslant$ 20 min at all pH values studied.

The specificity of the uptake to the SL (vs. SR) was routinely tested by repeating the experiment in the presence of 30 mM $Na^+$ ($Cl^-$) which shunts the active uptake via the $Na^+/Ca^{2+}$ exchanger (Ref. 29 and References therein). Active uptake persisting at 30 mM NaCl was due to small amounts of contaminating SR and was subtracted from the initial rate. The correction was negligible at low degrees of SL pump saturation and was $\leqslant$ 10% for $[Ca^{2+}]_0$ values up to 3-times the $K_m$ value for the CAM-activated pump. At that concentration the SL pump works at 98% of its maximal rate.

As will be shown below (Table I), the $K_m$ of the cardiac SR pump is 4.7-times that of the cardiac SL pump. The SR was in sufficient abundance to obtain a quantifiable uptake signal in the presence of 30 mM NaCl in the $[Ca^{2+}]_0$ range of 100 nM to 2 μM. In this range the SR pump expressed 13% to 96% of its maximal activity. Thus by extending the control experiments in the presence of 30 mM $Na^+$ to a much higher $[Ca^{2+}]_0$ range, it was possible to obtain kinetic data on the cardiac SR pump as a 'byproduct' of the present study. This was pursued for its comparative value. It was not possible to determine absolute rates for the cardiac SR because it was not possible to calibrate the CTC signal for this component. However, the ability to determine $K_m$ values was not affected since these do not require measurement of absolute rates.

*Determination of $H^+$ vs. $Ca^{2+}$ competition from pH dependence of $K_m$ for $Ca^{2+}$*

This method was developed for the $Ca^{2+}$-ATPase of rabbit skeletal SR in this laboratory [13]. Progress curves for active uptake are determined for a range of external $Ca^{2+}$ concentrations ($[Ca^{2+}]_0$) at selected pH values. The initial rate ($V_0$) data are analyzed to give maximal velocities at saturating $[Ca^{2+}]_0$ ($V_{max}$) and $K_m$ values defined as $[Ca^{2+}]_0$ where $V_0 = 1/2\ V_{max}$. Corresponding quantities are based on the maximal $[Ca^{2+}]_i$ observed in the plateau phase of the uptake curve in which a steady state is established between active uptake and passive leakage. These are $SS_{max}$ and the corresponding $K_m$. In the previous study of rabbit skeletal SR [13] strict parallelism was observed between the $V_0$-based and the steady state based values. The rabbit skeletal SR pump showed a high affinity for $Ca^{2+}$, with a $K_m$ for $Ca^{2+}$ of 73 nM at pH 7.0 and 30 °C.

Information concerning the role of $H^+$ in the reaction is obtained by determining the above parameters as a function of pH. The reciprocal of the $K_m$ ($1/K_m$) is identified with the apparent affinity of the cytoplasmically-oriented $Ca^{2+}$ binding site (translocator). In rabbit skeletal SR this parameter showed a dramatic pH dependence, decreasing by a factor of $10^3$ in the pH in the range of 8.0 to 5.5 [13]. Plots of $\log(1/K_m)$ vs. pH showed a shallow dependence (slope = 0.38) in the pH 7.0–8.0 range and a steep dependence (slope = 1.63) in

the pH 5.5 to 7.0 range, indicative of competition between $2H^+$ and 1 $Ca^{2+}$ for occupation of each of the two the cytoplasmically-oriented translocator sites. Analysis revealed a $pK_a$ for protonation close to the transition point at pH = 7.0 and suggested that the translocator site contained buried $COO^-$ groups (Ref. 13 or Fig. 5 of present paper).

## Results

The kinetics of the calmodulin (CAM)-activated form of the bovine cardiac SL pump were determined as a function of pH between 6.0 and 8.5 in the same manner as described earlier for the skeletal SR (Ref. 13; cf. Methods). Reactions were initiated by Mg-ATP addition at selected external $Ca^{2+}$ concentrations ($[Ca^{2+}]_o$) and pH values. The initial rates ($V_0$) of increase in the internal free $Ca^{2+}$ concentration ($[Ca^{2+}]_i$) and the maximal $[Ca^{2+}]_i$ in steady state (plateau phase) were determined. The $V_{max}$ and $SS_{max}$ were defined as the maxima of these respective values at saturating $[Ca^{2+}]_o$ values. Respective $K_m$ values were given by the $[Ca^{2+}]_o$ for 1/2 $V_{max}$ and 1/2 $SS_{max}$.

Fig. 1 shows pH dependence of $V_{max}$ and $SS_{max}$ values for the SL pump. Both parameters are maximal in the range 6.0–6.5, decreasing sharply in the 6.5–7.7 range, and showing minimal values for pH > 8.0. These findings are in agreement with the results reported by Caroni and Carafoli [3] with respect to the behavior in the alkaline range. That study reported a sharp drop in measured maximal velocity in the pH 7.0 to 6.0 range in apparent disagreement with the present findings. Three differences in protocol may be responsible for the difference between their results and ours: (a) Calmodulin concentration (ambient vs. saturating concentrations),

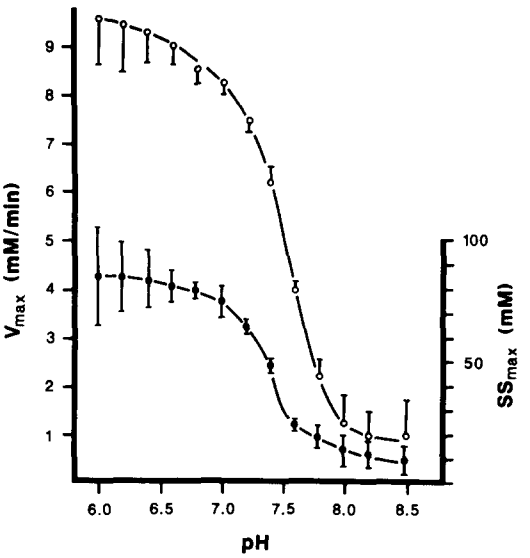


Fig. 1. pH dependence of $V_{max}$ and $SS_{max}$ of the CAM-activated form of the cardiac SL pump. Experimental details are given in Materials and Methods. Expressed in terms of mg protein, the maximal presented rate is 22.2 nmol/mg per min and the maximal steady-state uptake is 187 nmol/mg. Similar dependence was observed for the basal (unactivated) form of the pump (not shown), except that the absolute values were approx. 1/9th as large.

(b) buffer (impermeant vs. membrane permeant) and (c) species (canine vs. bovine).

The present $V_{max}$ and $SS_{max}$ values for pH 7.4 are in agreement with those previously reported for bovine cardiac SL (Table 1 of Ref. 29). Fig. 2 shows that the $V_{max}$ and $SS_{max}$ increase sharply with decreasing pH in the range 7.5 to 6.5, reaching a plateau for pH 6.5 to 6.0. The figure compares this with data for rabbit skeletal SR, showing close agreement between the two. Qualitatively the cardiac SR pump showed a similar tendency

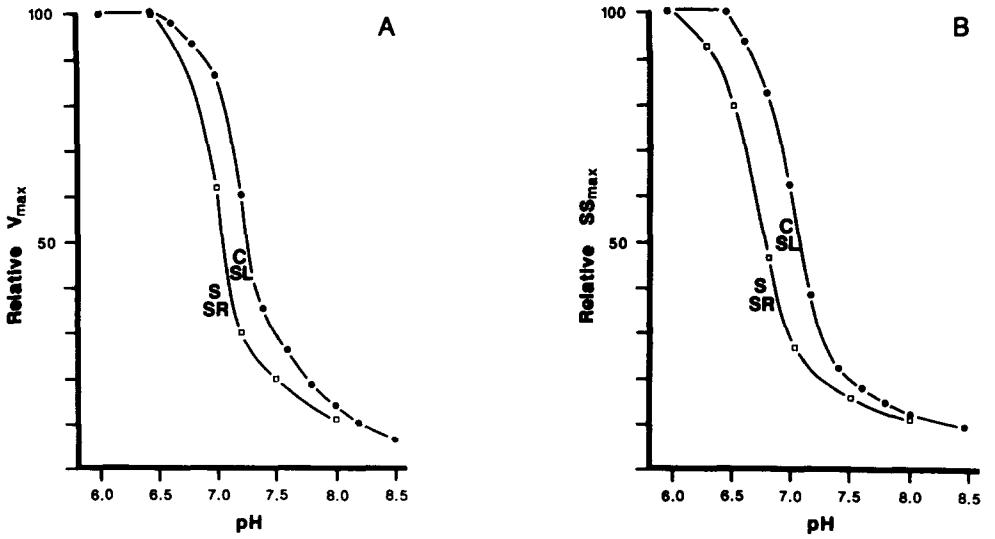


Fig. 2. Comparison of the pH dependence of $V_{max}$ (Panel A) and $SS_{max}$ (Panel B) for two $Ca^{2+}$-ATPase pumps. All curves are normalized to their maximum values observed at pH 6.0. Points (solid) denoted C-SL are for the CAM-activated cardiac SL pump are from Fig. 1. Data (squares) denoted S-SR are for the rabbit skeletal SR pump (at 30 °C) are from Ref. 13.

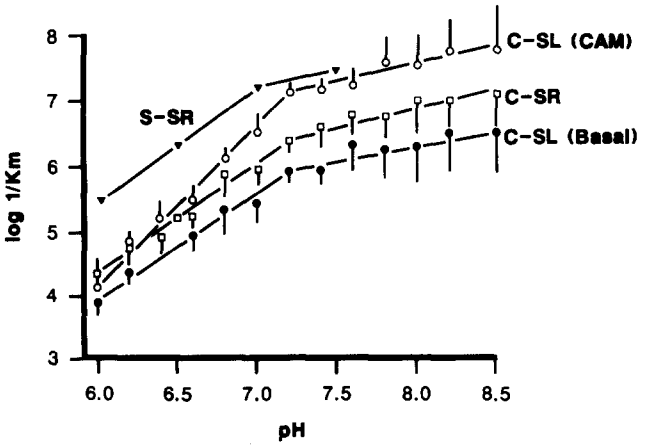


Fig. 3. The pH dependence of the apparent affinity ($1/K_m$ for transport velocity). The data are from the same experiments as in Fig. 2. Abbreviations are as in Fig. 2. Very similar behavior was observed for $K_m$ values based on maximal $[Ca^{2+}]_i$ achieved in the plateau phase (not shown). Alkaline values of skeletal SR [13] are omitted for clarity.

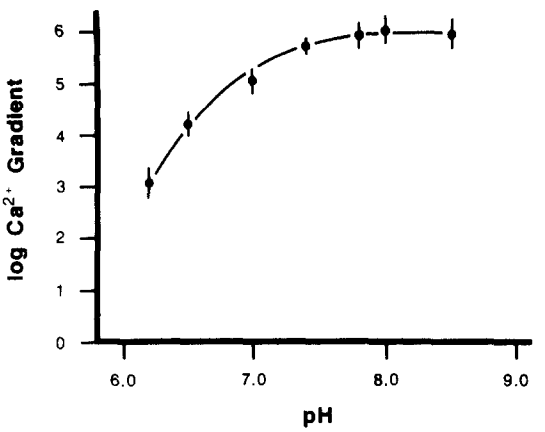


Fig. 4. The pH dependence of the $Ca^{2+}$ gradient ($[Ca^{2+}]_i/[Ca^{2+}]_o$) generated by the CAM activated SL enzyme. The gradient was evaluated at $[Ca^{2+}]_o$ equal to the $K_m$ appropriate to each pH.

but the $V_{max}$ vs. pH data could not be presented due to our inability to calibrate this component in the present experimentation. Other studies have reported that canine cardiac SR has maximal rates at pH 6.2–6.4 [20].

The pH dependence of the $K_m$ for $Ca^{2+}$ was also determined in the present study. Fig. 3 shows these data for the pH range 6.0–8.5. Since the pump shows an approx. $10^4$-fold change in $K_m$ over this range, the data are displayed as the logarithm of the apparent $Ca^{2+}$ affinity ($\log(1/K_m)$). The CAM-activated cardiac SL enzyme shows high affinity and a low pH dependence in the alkaline range, with a slope of 0.54. Below pH 7.2, the pump shows a greater pH dependence, with a slope of 2.6. The cardiac SR pump shows similar behavior, except that the absolute $K_m$ values are lower and the slope in the acid range is lower. For the basal state of the cardiac SL pump, the absolute values are still lower. Previous data from the skeletal SR pump [13] are also presented. Table I lists the $K_m$ values at pH 7.4, slopes in the acid and alkaline and acid ranges, and pH values of the transition points. Quantitative differences between these four species will be considered in more detail in the next section.

The present study also yielded information on the pH dependence of the maximal $Ca^{2+}$ gradients produced by the cardiac SL pump. Fig. 4 shows the pH dependence of the maximal gradient produced at $[Ca^{2+}]_o = K_m$. The figure reveals a dependence similar to that observed for the skeletal SR pump, with maximal gradients of $10^6$ observed in the alkaline range. Gradients produced by the pump in the basal condition (not shown) are much lower, being degraded by the process of passive leakage.

TABLE I

*Comparison of pH dependence of CAM-activated and basal states of the cardiac SL pump*

| Enzyme | State | $K_m$ at pH 7.4 (nM) | Trans. pH | Slope | |
|---|---|---|---|---|---|
| | | | | acid | alkaline |
| Cardiac SL | CAM-act. | 48 (64)[a] (33– 67)[b] | 7.2 | 2.6 | 0.5 |
| Cardiac SL | basal | 1000 (1800)[a] (570–1800)[b] | 7.2 | 1.7 | 0.5 |
| Cardiac SR | – | 304 (220– 419)[b] | 7.2 | 1.7 | 0.6 |
| Skeletal SR[c] | – | 36 (22– 57)[b] | 7.0 | 1.6 | 0.4 |

[a] Value from Ref. 29.
[b] Range encompassing one standard deviation.
[c] Values from Ref. 13 (30 °C).

## Discussion

The most important observation in the present study is the striking similarity in the pH dependence of the $K_m$ values of the cardiac SL pump, the cardiac SR pump and the previously-studied skeletal SR pump. This has several implications: (a) It demonstrates a direct competition between 4 $H^+$ and 2 $Ca^{2+}$ for the high-affinity $Ca^{2+}$ binding sites. (b) It adds to the emerging picture of $Ca^{2+}$-ATPase pumps working by a common mechanism of $Ca^{2+}/H^+$ or $M^+$ counter-transport. (c) It suggests that in beating heart experiencing ischemia and acidosis, there will be a drop in $K_m$ for both the processes of $Ca^{2+}$ extrusion and $Ca^{2+}$ accumulation. We will first consider the meaning of our results with respect to the structure of the high-affinity $Ca^{2+}$ binding (translocator) site.

*Evidence that the high-affinity binding site of cardiac SL pump contains $COO^-$ groups*

Fig. 3 shows that there is direct competition between $H^+$ and $Ca^{2+}$ as expressed in the rate of transport and reflected in the pH dependence of the $K_m$ for $Ca^{2+}$. Below pH 7.2 there is a 1.7 or 2.6 order of magnitude drop in apparent $Ca^{2+}$ affinity for each unit decrease in pH (basal or CAM-activated form, respectively). The transition pH (Table I) is appropriate for the $pK_a$ of $COO^-$ groups in a non-polar environment or in close proximity to eachother. A suitable model compound illustrating this principle is EGTA (Ref. 34). A slope of 2.0 (Fig. 3) is predicted for 2 $H^+$ competing with 1 $Ca^{2+}$ or for 4 $H^+$ competing with 2 $Ca^{2+}$. The latter is preferred since analysis of the Hill coefficient for $Ca^{2+}$ predicts a stoichiometry of 2 $Ca^{2+}$ removed per transport event [29] and analysis of the gradients produced as a function of $[ATP]/([ADP] \cdot [P_i])$ ratio predicts 2 $Ca^{2+}$ moved per ATP split [35].

The above conclusion is very reasonable in light of recent molecular genetic investigations of the skeletal SR enzyme, the deduced amino acid sequence of the cardiac SL enzyme, and the strength of the analogy between the several $Ca^{2+}$-ATPase pumps. As related in the Introduction, the probable high-affinity binding site has been described for rabbit skeletal SR. Clarke et al. [15] have performed molecular cloning experiments using site-directed mutagenesis to identify amino acid residues critical to $Ca^{2+}$-dependent phosphorylation by ATP but not critical to phosphorylation by high con-

TABLE II

*Comparison of proposed high-affinity calcium binding sites for SR and plasma membrane calcium pumps*

Data for SR, skeletal and cardiac were taken from Refs. 14 and 27 using the numbering of the former. Comparison of these two publications shows homology between the skeletal/fast twitch and cardiac/slow twitch sequences about the amino acids listed above. Data for SL, skeletal and cardiac were taken from Fig. 3 of Ref. 30 (cf. Ref. 36), using the numbering system for the PMCA2 form. That figure shows homology between the PMCA2 form (derived from brain and heart) and the PMCA1 form (derived from brain and skeletal muscle), about the amino acids listed above. Data for PM, erythrocyte are taken from Fig. 4 of Ref. 31. They show a very high degree of homology with that of SL, skeletal and cardiac about the above-listed sites. The assignments to Sites 1–6 were based on Table 2 of Ref. 15 except that a proximal asparagine of the SL and PM enzymes was considered by us a better candidate that an alanine for Site 2. Residues and values in parentheses are, in our opinion, possible candidates for participation.

| Site | Type of calcium ATPase | Amino acid and number | Number of | |
|---|---|---|---|---|
| | | | $COO^-$ | oxygens |
| 1 | SR, skeletal & cardiac | E309 | 1 | 2 |
| | SL, skeletal & cardiac | E412 | 1 | 2 |
| | PM, erythrocyte | E423 | 1 | 2 |
| 2 | SR, skeletal & cardiac | E771[a], (N768[a]) | 1 | 2 (3) |
| | SL, skeletal & cardiac | –, N841, (D857) | 0 (1) | 0 (3) |
| | PM, erythrocyte | –, N851, (D867) | 0 (1) | 0 (3) |
| 3 | SR, skeletal & cardiac | N796[a] | 0 | 1 |
| | SL, skeletal & cardiac | N869 | 0 | 1 |
| | PM, erythrocyte | N879 | 0 | 1 |
| 4 | SR, skeletal & cardiac | T799[a] | 0 | 1 |
| | SL, skeletal & cardiac | T874[b] | 0 | 1 |
| | PM, erythrocyte | T884 | 0 | 1 |
| 5 | SR, skeletal & cardiac | D800[a] | 1 | 2 |
| | SL, skeletal & cardiac | D873[b] | 1 | 2 |
| | PM, erythrocyte | D883 | 1 | 2 |
| 6 | SR, skeletal & cardiac | E908[a] | 1 | 2 |
| | SL, skeletal & cardiac | N955 | 0 | 1 |
| | PM, erythrocyte | N965 | 0 | 1 |
| (7) | SR, skeletal & cardiac | (S902[a]), (T906[a]) | 0 | 2 |
| | SL, skeletal & cardiac | E948, (H949), T951 | 1 | 3 |
| | PM, erythrocyte | S957, (Q958), T961 | 0 | 2 |
| Totals | | | | |
| | SR, skeletal & cardiac: | | 4 | 10 (13) |
| | SL, skeletal & cardiac: | | 2 (4) | 7 (13) |
| | PM, erythrocyte: | | 2 (3) | 7 (12) |

[a] This value was incremented by 1 to bring about agreement with the numbering in Ref. 15.
[b] Assignments to sites 4 and 5 were exchanged for this residue.

centrations of $P_i$. These experiments identified the following amino acids as being critical to the high-affinity $Ca^{2+}$ binding site of rabbit skeletal SR: E(Glu)309, E(Glu)771, N(Asn)796, T(Thr)799, D(Asp)800 and E(Glu)908. This grouping of amino acids has four $COO^-$ groups and a total of 10 oxygens which could participate in the liganding of 2 $Ca^{2+}$. As noted above, our previous finding of 4 $H^+$ vs. 2 $Ca^{2+}$ competition for the skeletal SR enzyme is in good agreement with this.

The sequence information for the rabbit skeletal SR enzyme can be readily used to identify candidate amino acid residues for the other forms of the enzyme, including the cardiac SL. Clarke et al. [15] compared their sequence with published sequences for rat plasma membrane (PM) $Ca^{2+}$-ATPase [36] and three other transport ATPases and suggested equivalences between certain amino acids. The group reporting the rat brain PM $Ca^{2+}$-ATPase sequence [36] has more recently published very similar sequences deduced for sarcolemmal $Ca^{2+}$ pump from clones with DNA derived from heart and skeletal muscle [30]. There was a high degree of homology between the rat PM, and skeletal and cardiac SL $Ca^{2+}$-ATPases. In Table II we present these data based on the equivalences suggested by Clarke et al. [15]. The table also presents potential seventh site. The table also presents data for the erythrocyte PM $Ca^{2+}$-ATPase which also shows a high degree of homology with the other forms. Around the seven sites listed, there is a high degree of homology between the skeletal and cardiac SL and erythrocyte PM pump sequences. The homology between these and the SR pumps depends upon the site considered. It was high for Site 1 and was absent for Site 6. For Sites 3–5 homology is present with respect to the placement of N and D residues but not with respect to the placement of T. In the SR sequence T is one digit lower than D. In the SL and PM sequences it is one digit higher.

The table shows that the sequence identified as prevalent in cardiac SL can have as many as four $COO^-$ groups in the region proposed for the high-affinity binding site. This would be sufficient for 4 $H^+$ vs. 2 $Ca^{2+}$ competition and for a slope of 1.7 in Fig. 3, as seen for the unactivated enzyme. The slope of 2.6 seen for the CAM-activated enzyme can be explained as the summation of this effect and a $H^+$ vs. $Ca^{2+}$ competition for occupation of CAM. The table also shows that as many as 13 oxygens could be available for liganding the two $Ca^{2+}$. This is ample to meet the apparent requirement of 5–6 oxygens per $Ca^{2+}$ for high-affinity binding.

*Application of $H^+/Ca^{2+}$ competition and counter-transport model to the $Ca^{2+}$-ATPases*

Fig. 5 depicts a model involving a $H^+$ and $Ca^{2+}$ binding site (translocator) which is capable of explaining the $K_m$ and $V_{max}$ effects observed for the four pump species of the present study. This model was first proposed for the skeletal SR pump [13]. For simplicity of visualization, only one of the two translocator (high-affinity $Ca^{2+}$ binding) sites is depicted. Likewise, the uncharged oxygen ligands are not depicted. The model depicts a series of states of the translocator as the pump goes through its cycle (clock-wise direction). In the states at the top of the figure, the translocators are 'outwardly'-oriented (*cis*, or cytoplasmically oriented).

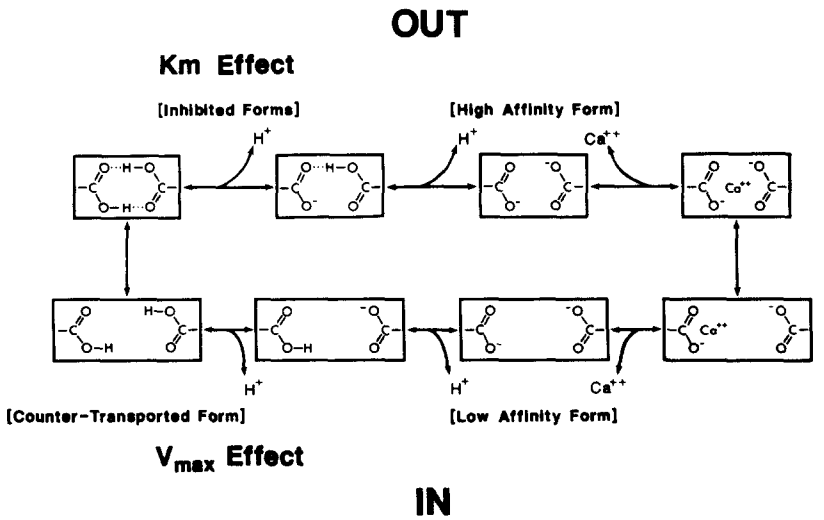


Fig. 5. Model of $Ca^{2+}$ binding site showing $H^+/Ca^{2+}$ competition. A similar model was proposed for skeletal SR pump [13]. Each $Ca^{2+}$ binding site contains two $COO^-$ groups. Each pump contains two translocator sites which transform from 'outward' and 'inward' orientation. Transport proceeds in the clockwise direction. Orientation is with respect to the inside-out vesicles studied. 'Out' represents the cytoplasmic side; 'In' represents the extracellular side. Binding of $H^+$ on the outwardly-oriented translocator raises the apparent $K_m$ for $Ca^{2+}$. Binding of $H^+$ to the inwardly-oriented translocator is necessary for return to outward orientation and for completion of the cycle. Thus $H^+$ occupation of the inwardly-oriented translocator determines the $V_{max}$.

At the bottom they are 'inwardly'-oriented (*trans*, or lumenally or extra-cellularly oriented).

Competition between $Ca^{2+}$ and $H^+$ for occupancy of the cytoplasmically-oriented translocator (top) has already been described herein. The model also describes competition for the extra-cellularly oriented translocator. After phosphorylation of the enzyme and reorientation of the translocators, the $COO^-$ groups are more widely separated, leading to a drop in $Ca^{2+}$ affinity. At high *trans* $Ca^{2+}$ concentrations, $Ca^{2+}$ removal becomes limiting to the overall rate [13]. According to the model, *trans* $H^+$ assists in this by the mechanism of $H^+$ vs. $Ca^{2+}$ competition and serves as a counter-transported species. In the alkaline range $Ca^{2+}$ removal and return constitute rate limitations, thus explaining the pH dependence of the $V_{max}$.

The model of Fig. 5 has significant predictive value. Computer modelling studies [13,17,18] based on the model correctly reproduced both the $10^3$-fold variation of $K_m$ and the $>10$-fold variation $V_{max}$ with pH. The computer models were based on the model of Fig. 5 and on a large amount of mechanistic information from a number of laboratories involving phosphorylation and dephosphorylation kinetics. Final calculations [17,18] were made to a rigorous standard using literature values or estimated rate constants for all steps in the cycle. Once determined, these constants were not varied as the pump dependence on diverse factors such as $H^+$, $K^+$, $Mg^{2+}$, Mg-ATP, ADP and $P_i$ concentration was simulated. In the model, the mathematical product of the equilibrium constants of every step of the cycle conformed to the theoretical (and experimentally-verified) equilibrium constant of the cycle. The latter was equal to the $K_{eq}$ for ATP hydrolysis. The model was not 'open-ended'. The only assumption made was that the various forms of the enzyme achieved steady-state. The model reproduced the skeletal SR data shown in Figs. 2 and 3.

The striking similarities in pH dependence of the four species (Figs. 2 and 3) suggest that the $H^+/Ca^{2+}$ competition mechanism of Fig. 5 is common to all of the above-mentioned pumps. The molecular genetic experimentation discussed above provides a structural basis for considering this phenomenon. The modeling experiments with skeletal SR provide a kinetic framework for considering $Ca^{2+}$-ATPase behavior. Table III summarizes significant properties of the skeletal SR, cardiac SR, cardiac SL and erythrocyte PM $Ca^{2+}$-ATPase pumps. The following sections will discuss similarities and differences observed with respect to translocator behavior.

*Cardiac SR pump vs. skeletal SR pump*

The pH dependence of the cardiac SR pump conforms to that of the skeletal SR pump and the model of Fig. 5. The behavior of the cardiac SR pump is complicated by the action of the endogenous modifier, phospholamban, which can be phosphorylated in cAMP-

TABLE III

*Comparison of characteristics of SR and plasma membrane calcium pumps*

Skeletal SR data are for rabbit [13]. Experimentation (30 °C) defining its counter-transported ions and absence of membrane potential ($E_m$) effects is given in Refs. 16, 37 and 38. The equilibrium constant of the overall reaction ($K_{eq}$) was presented in Ref. 39. Cardiac SR data are for canine species, pH 7.0 [24]. Cardiac SL data are for bovine species at 37 °C. Data are taken from Ref. 29 ($K_m$), Ref. 38 (counter-transport and insensitivity to $E_m$) and Ref. 35 ($K_{eq}$). Red cell PM (human) data are from Ref. 40, or as indicated. n.s. means not studied.

| Type | Stoich. | Activator | $K_m$ (nM) | Counter-ion | $K_{eq}$ (M) ($\times 10^6$) | $E_m$ effect |
|---|---|---|---|---|---|---|
| Skeletal SR | 2 | None | 73 | $K^+$, $H^+$ | 9.02 | negligible |
| Cardiac SR | 2 | Basal | 942 | N.S. | N.S. | N.S. |
| | | cAMP phos. | 617 | | | |
| | | CAM phos. | 526 (304) [a] | | | |
| | | cAMP+CAM phos. | 417 | | | |
| Cardiac SL | 2 | Basal | 1800 | $H^+$ | 15 | negligible |
| | | cAMP phos. | 1100 | | | |
| | | CAM | 64 | | | |
| | | cAMP+CAM | 63 | | | |
| Red cell PM | 1.6 (0.9) | Basal | 400 | $H^+$ [b] | N.S. | N.S. |
| | | CAM | 800 (200) [c] ($\approx$ 500) [d] | | | |

[a] From the present study.
[b] From Ref. 41.
[c] From Ref. 42.
[c] From Ref. 43.

and CAM-dependent processes. The data compiled in Table III show that even after complete activation, the $K_m$ of the cardiac SR pump is 4–6-fold larger than that of skeletal SR. Detailed inspection of the published data as well as our own experimentation, shows that the difference does not arise from the choice of Ca-EGTA constants or experimental conditions. It is of interest that there is a high degree of homology between the two enzymes about the six amino acids of the binding sites proposed by Clarke et al. [15]. It would thus seem that differences in other parts of the enzyme are responsible for the difference in apparent affinity.

It should be noted that the $K_m$ values are not strictly identical to $Ca^{2+}$ dissociation constants of the high-affinity sites. Differences are expected since the $K_d$ is an equilibrium constant while the $K_m$ is a kinetically-derived constant. For example, Inesi et al. [44,45] analyzed passive binding to the rabbit skeletal SR enzyme and showed it to be cooperative with a Hill coefficient of 1.82 and an association constant of $2.3 \cdot 10^6$ $M^{-1}$. This corresponds to a $K_d$ of 430 nM. However, the actual $K_m$ is 73 nM (Ref. 13; Table III this publication) or 5.9-fold lower. Computer modelling experiments [18] showed that $K_m$ values can be lower than $K_d$ values if the equilibrium constants of the subsequent phosphorylation and translocation reactions are greater than 1.0. The computer modeling experiments showed that use of the passive $Ca^{2+}$ binding constants [44,45], an equilibrium constant of 1.0 for the phosphorylation step and an equilibrium constant 14 for the 'outward'-to-'inward' (Fig. 5) reorientation step yields correct values of $K_m$. We suggest that it will be most productive to consider the $K_m$ values of the cardiac SR pump in its various states of activation in relationship to emerging information on the effect of phospholamban on enzyme phosphorylation and dephosphorylation kinetics within its cycle.

*Comparison of cardiac SL pump with other pumps*

Observations relevant to the comparison of the cardiac SL pump with the other pumps are summarized in Table III. Kinetic and thermodynamic analysis of the cardiac SL pump shows that two $Ca^{2+}$ are moved per transport event [29] and gives strong evidence for a stoichiometry of two $Ca^{2+}$ moved per ATP split. The overall equilibrium constant of the pump is correct for a stoichiometry of 2 $Ca^{2+}$ per ATP [35]. In addition to the 4 $H^+$ vs. 2 $Ca^{2+}$ competition described herein, other studies have shown $H^+$ involvement in the pump cycle. Studies [29,38] manipulating the internal ion composition suggest that $H^+$ is counter-transported and show that the pump is not sensitive to imposed membrane potential ($E_m$). The cardiac SL pump is indifferent to alkali cations in the lumen. This represents a significant difference with the skeletal SR pump, which is sensitive to $K^+$ and other monovalent cations [13,16,18]. It will be interesting to consider such differences in terms of the differences in primary structure described in Table II.

The most interesting difference between the cardiac SL pump and the other pumps is its poor performance absence of CAM. Its basal state has a 1.8 $\mu$M $K_m$ and a very low $V_{max}$ indicative of a low turnover number [29]. In contrast, the CAM-activated form of the cardiac SL pump shares with the skeletal SR pump the highest apparent $Ca^{2+}$ affinity (Fig. 3, Table I). The two species also show nearly identical transition point and pH dependence in the alkaline range (Table I). The greater pH sensitivity of the CAM-activated form of the SL pump in the acidic range can be accounted for by $H^+$ binding to CAM. Protonation behavior of CAM has been described [46]. It will be useful to determine the mechanism by which Ca-CAM increases the apparent $Ca^{2+}$ affinity. Possible mechanisms are (a) an allosteric effect on the passive binding reaction, (b) alteration of the rate or equilibrium constant for pump phosphorylation [29], or (c) mechanisms by which CAM delivers $Ca^{2+}$ to the translocator site.

One would expect that the erythrocyte PM pump would show a high degree of similarity to the cardiac SL pump, since the two subserve the same function. A $Ca^{2+}/H^+$ exchange mechanism has been proposed for the mechanism of the erythrocyte PM pump [41]. The two pumps have a high degree of homology about Sites 1–6 of Table I. However, the erythrocyte PM pump has a lower $Ca^{2+}$ affinity in the CAM-activated state. Existing information on the $Ca^{2+}$ dependence of the erythrocyte PM pump puts its $K_m$ in the range of cardiac SR. There are also differences in sequence about Site 7 for the two pumps.

*Physiological significance of differences between cardiac SR and SL pumps*

The present study has demonstrated that the cardiac SR pump has a substantially higher $K_m$ for $Ca^{2+}$ than does the CAM-activated form of the SL pump. While comparisons between other studies would seem to suggest this, the present study proves this by direct comparison in the same tissue, with the same preparations, under precisely the same experimental conditions using the same $Ca^{2+}$-EGTA constants. We propose that the 5-fold difference in $K_m$ has a physiological basis in the different roles played by the two pumps in the contraction/relaxation cycle. The SR pump must reaccumulate released $Ca^{2+}$ but there is no compelling need for it to continue to function during the end diastolic phase. The reaccumulation is well served by a pump with a $K_m$ of 304 nM and a Hill coefficient of about 2. The pump would work at maximal rates against high $[Ca^{2+}]_{cyt}$, but would drop to 0.1 $V_{max}$ at $[Ca^{2+}]_{cyt} = 100$ nM. In contrast to this, the SL pump is best positioned to set the end diastolic $[Ca^{2+}]_{cyt}$. This function is well served by a

pump with a $K_m$ of 64 nM and a Hill coefficient of 3.7. The pump would work at $\geqslant 0.84\ V_{max}$ and $[Ca^{2+}]_{cyt} \geqslant$ 100 nM, but would slow down abruptly if $[Ca^{2+}]_{cyt}$ approached its $K_m$ of 64 nM. We believe that these properties will also prove sufficient to explain a number of cardiac phenomena such as the 'staircase effect'. Such indirect interactions between the two pumps should be amenable to computer modelling.

*Significance for ischemia and acidosis*

A second physiological implication of our findings involves the pH dependence of the pumps. There is general agreement that the combined effects of high cytoplasmic $Ca^{2+}$ levels and low pH are instrumental in causing irreversible damage accompanying myocardial infarction in man [47,48]. Measurements of internal pH in ischemia or coronary occlusion of animal hearts have given values as low as 6.2 [49] or 6.5 [50]. Irreversible effects in man probably do not require such an extreme perturbation. The combined effects of reduced ATP, increased depolarization and $Ca^{2+}$ influx, and increased demand for ATP by ion-handling pumps and by the contractile machinery, results in a self-sustaining cycle of energy misuse which can end in cell death [47,48]. The SL $Ca^{2+}$ pumping ATPase plays a crucial role in countering this cycle. It is important to consider the quantitative implications of the pH dependence of the $V_{max}$ and $K_m$.

Increasing acidity has two opposing effects on the cardiac SL pump: (a) raising its $V_{max}$ and (b) lowering its $Ca^{2+}$ affinity. The relative importance of these two effects depends upon the cytoplasmic $Ca^{2+}$ concentration ($[Ca^{2+}]_{cyt}$). Fig. 6 shows the rate of the pump as a function of pH at selected $[Ca^{2+}]_{cyt}$ ($=[Ca^{2+}]_o$) levels ranging from 100 nM to 10 $\mu$M. The horizontal dashed line indicates the level expected for pump working under normal conditions (pH 7.4) against cytoplasmic $Ca^{2+}$ at an assumed and diastolic level of 100 nM. The figure shows that the initial effect of acidosis is to

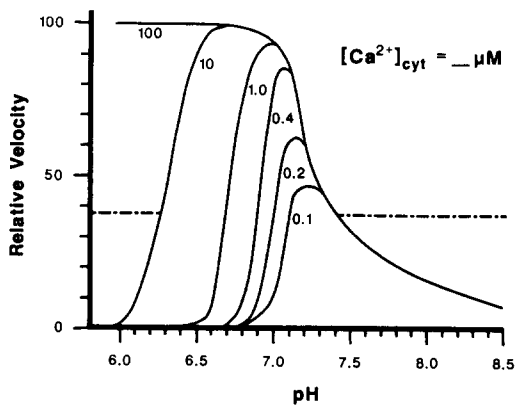


Fig. 6. The pH dependence of velocity of the CAM-activated SL pump at selected $[Ca^{2+}]_{cyt}$ values. The curves were calculated from the data of Figs. 2 and 3.

increase pump rates, as evidenced by the negative slope of all of the lines in the pH 7.2–7.4 range. This is the result of the dominance of the $V_{max}$ effect over the $K_m$ effect. As the pH is further reduced, all curves plateau and decline. At this point the $K_m$ effect becomes stronger than the $V_{max}$ effect. The pH of the transition ('pH optimum') decreases with increasing $[Ca^{2+}]_{cyt}$, ranging between 7.2 and 6.6 for 100 nM $\leqslant [Ca^{2+}]_{cyt} \leqslant 10$ $\mu$M. Inasmuch as elevated $[Ca^{2+}]_{cyt}$ is correlated with lowered pH in ischemia, the pump is expected to continue to make substantial contributions to $Ca^{2+}$ removal during increasing acidosis. However, Fig. 6 predicts that as the internal pH drops from its normal level of approx. 7.2 [51] to values of less than 6.8, its ability to lower $[Ca^{2+}]_{cyt}$ to values below 400 nM will be seriously compromised.

Langer [52] has shown that decreasing pH decreases the total $Ca^{2+}$ associated with heart cells and fit his data to an empirical equation. It would be useful to model total cellular $Ca^{2+}$ and $[Ca^{2+}]_{cyt}$ in terms of differential equations based on the known properties of the elements of the system responsible for transport and permeability: (a) the $Ca^{2+}$-pumping ATPase of the SL, (b) the $Na^+/Ca^{2+}$ exchanger, (c) the leaks and gated channels of the SL, (d) the $Ca^{2+}$-pumping ATPase of the SR, and (e) the leaks and gated channels of the SR. For this purpose, it would be useful to have information on the pH dependence of each of these systems. For example, one study has shown that the rate of the $Na^+/Ca^{2+}$ exchanger is decreased at pH 6.0 [53]. Modelling the effects of acidosis on cardiac contractility [52,54] will be still more complicated because the $Ca^{2+}$ sensitivity of the contractile machinery decreases with acid pH [11].

## Acknowledgements

This work was supported by USPHS GM 23990, HL 07188, HL 38228 and by a grant from the American Heart Assn., Florida Affiliate. We thank Dr. Arthur L. Bassett for interesting discussions and for a critical reading of the manuscript. We thank Drs. David MacLennan and Gary Shull for their helpful responses to our queries.

## References

1 Fabiato, A. (1985) J. Gen. Physiol. 85, 189–320.
2 Caroni, P. and Carafoli, E. (1980) Nature 283, 765–767.
3 Caroni, P. and Carafoli, E. (1981) J. Biol. Chem. 256, 3263–3270.
4 Caroni, P. and Carafoli, E. (1981) J. Biol. Chem. 256, 9371–9373.
5 Carafoli, E. (1988) J. Cardiovasc. Pharmacol. 12, S77–S84.
6 Reeves, J.P. and Sutko, J.L. (1979) Proc. Natl. Acad. Sci. USA 76, 590–594.
7 Pitts, B.J.R. (1979) J. Biol. Chem. 254, 6232–6235.
8 Gaskell, W.H. (1880) J. Physiol. (London) 3, 48–75.
9 Cingolani, H.E., Mattiazzi, A.R., Blesa, E.S. and Gonzalez, N.C. (1970) Cir. Res. 26, 269–278.

10 Katz, A.M. (1977) Physiology of the Heart, pp. 419–433, Raven Press, New York.
11 Fabiato, A. and Fabiato, F. (1978) J. Physiol. (London) 276, 233–255.
12 Murphy, A.J. (1981) J. Biol. Chem. 256, 12046–12050.
13 Haynes, D.H. and Mandveno, A. (1983) J. Membr. Biol. 74, 25–40.
14 MacLennan, D.H., Brandl, C.J., Korczak, B. and Green, N.M. (1985) Nature 316, 696–700.
15 Clarke, D.M., Loo, T.W., Inesi, G. and MacLennan, D.H. (1989) Nature 339, 476–478.
16 Chiu, V.C.K. and Haynes, D.H. (1980) J. Membr. Biol. 56, 219–239.
17 Haynes, D.H. and Mandveno, A. (1984) Comput. Biomed. Res. 17, 143–162.
18 Haynes, D.H. and Mandveno, A. (1987) Physiol. Rev. 67, 244–284.
19 Mandel, F., Kranias, E.G., De Gende, A.G., Sumida, M. and Schwartz, A. (1982) Circ. Res. 50, 310–317.
20 Tate, C.A., Bick, R.J., Chu, A., Van Winkel, W.B. and Entman, M.L. (1985) J. Biol. Chem. 260, 9618–9623.
21 Davis, B.A., Schwartz, A., Samaha, F.J. and Kranias, E.G. (1983) J. Biol. Chem. 258, 13587–13591.
22 Mas-Oliva, J.M., DeMeis, L. and Inesi, G. (1983) Biochemistry 22, 5822–5825.
23 Kirchberger, M.A., Tada, M. and Katz, A.M. (1974) J. Biol. Chem. 249, 6166–6173.
24 Kranias, E.G. (1985) Biochim. Biophys. Acta 844, 193–199.
25 Tada, M., Ohmori, F., Yamada, M. and Abe, H. (1979) J. Biol. Chem. 254, 319–326.
26 Tada, M., Yamada, M., Ohmori, F., Kuzuya, T., Inui, M. and Abe, H. (1980) J. Biol. Cem. 255, 1985–1992.
27 Brandl, C.J., Green, N.M., Korczak, B. and MacLennan, D.H. (1986) Cell 44, 597–607.
28 Trumble, W.R., Sutko, J.L. and Reeves, J.P. (1980) Life Sci. 27, 207–214.
29 Dixon, D.A. and Haynes, D.H. (1989) J. Biol. Chem. 264, 13612–13622.
30 Greeb, J. and Shull, G.E. (1989) J. Biol. Chem. 264, 18569–18576.
31 Strehler, E.E., James, P., Fischer, R., Heim, R., Vorherr, T., Filoteo, A.G., Penniston, J.T. and Carafoli, E. (1990) J. Biol. Chem. 265, 2835–2842.
32 Dixon, D., Brandt, N. and Haynes, D.H. (1984) J. Biol. Chem. 259, 13737–13741.
33 Millman, M.S., Caswell, A.H. and Haynes, D.H. (1980) Membr. Biochem. 3, 291–315.
34 Martell, A.E. and Smith, R.M. (1974) Critical Stability Constants, Vol. F: Amino Acids, Plenum Press, New York.
35 Dixon, D.H. and Haynes, D.H. (1990) J. Bioenerg. Biomembr. 22, 181–195.
36 Shull, G.E. and Greeb, J. (1988) J. Biol. Chem. 263, 8646–8657.
37 Haynes, D.H. (1982) Arch. Biochem. Biophys. 215, 444–461.
38 Dixon, D.A. and Haynes, D.H. (1989) J. Membr. Biol. 112, 169–183.
39 Trevorrow, K. and Haynes, D.H. (1984) J. Bioenerg. Biomembr. 16, 53–59.
40 Waisman, D.M., Gimble, J.M., Goodman, D.B.P. and Rasmussen, H. (1981) J. Biol. Chem. 256, 409–414.
41 Smallwood, J.I., Waisman, D.M., Lafreniere, D. and Rasmussen, H. (1983) J. Biol. Chem. 258, 11092–11097.
42 Muallem, S. and Karlish, S.J.D. (1982) Biochim. Biophys. Acta 687, 329–332.
43 Niggli, V., Adunyah, E.S. and Carafoli, E. (1981) J. Biol. Chem. 256, 8588–8592.
44 Inesi, G., Kuzmack, M. and Verjovski-Almeida, S. (1978) Ann. N.Y. Acad. Sci. 307, 224–232.
45 Inesi, G., Kurzmack, M., Coan, C. and Lewis, D.E. (1980) J. Biol. Chem. 255, 3025–3031.
46 Iida, S. and Potter, J.D. (1986) J. Biochem. 99, 1765–1772.
47 Hearse, D.J. (1979) in Enzymes in Cardiology: Diagnosis and Research (Hearse, D.J. and De Leiris, J., eds.), pp. 1–19, John Wiley & Sons, New York.
48 Jennings, R.B. and Reimer, K.A. (1979) in Enzymes in Cardiology: Diagnosis and Research (Hearse, D.J. and De Leiris, J., eds.), pp. 21–57, John Wiley & Sons, New York.
49 Garlick, P.B., Radda, G.K. and Seeley, P.J. (1979) Biochem. J. 184, 547–554.
50 Rehr, R.B., Clarke, G., Tatum, J., Lower, R. and Wetstein, L. (1987) Clin. Res. 35, 5a.
51 Bountra, C., Kaila, K. and Vaughan-Jones, R.D. (1988) J. Physiol. 398, 341–360.
52 Langer, G.A. (1985) Circ. Res. 57, 374–382.
53 Philipson, K.D., Bersohn, M.M. and Nishimoto, A. (1982) Circ. Res. 50, 287–293.
54 Langer, G.A., Rich, T.L. and Ji, S. (1989) Circ. Res. 65, 894–902.